MULTI-THRESHOLD TOP — FULL-DIVERSITY VECTOR PERTURBATION PRECODING WITH FINITE-RATE FEEDFORWARD

Johannes Maurer, Joakim Jaldén, and Gerald Matz

Institute of Communications and Radio-Frequency Engineering, Vienna University of Technology
Gusshausstrasse 25/389, A-1040 Vienna, Austria
phone: +43 1 58801 38968; fax: +43 1 58801 38999; email: jmaurer@nt.tuwien.ac.at

Abstract – We consider vector perturbation (VP) precoding for a multiple antenna broadcast scenario with multiple non-cooperative users. Under an instantaneous transmit power constraint, VP precoding requires the feedforward of a power normalization factor to the users. Simple quantization of the power normalization factor is shown to result in an error floor. To overcome this problem, we propose a new precoding scheme that uses a finite set of power normalization factors and avoids transmission at all when the available power is not sufficient to perform channel equalization at the transmit side. With this scheme, full diversity can be achieved (even with imperfect channel state information) while simultaneously significant amounts of transmit power can be saved.

1. INTRODUCTION

Background. In this paper, we study a wireless broadcast scenario in which a base station equipped with multiple antennas transmits simultaneously to multiple non-cooperative users. In this context, vector perturbation (VP) precoding [1–3] is a promising technique with regard to performance and complexity. The main idea is to perform channel inversion ("pre-equalization") at the base station in combination with a perturbation of the transmit vector in order to maximize receive SNR [2]. The receivers detect their data symbols by scaling the received signals, followed by a modulo operation and scalar symbol detection. Throughout the paper, we will refer to this scheme as *conventional VP precoding*. To meet an instantaneous or short-term transmit power constraint, the base station has to perform adaptive power normalization. Unfortunately, the corresponding power normalization factor has to be known by the receivers for the purpose of detection.

Contributions. The contributions in this paper are as follows:

- We discuss a straightforward feedforward scheme for conventional VP precoding that uses single-user beamforming to transmit the quantized power normalization factor to the users; we show that with this simple scheme the quantization of the power normalization factor results in a mismatch at the receivers and hence in an undesired error floor.
- We propose an alternative precoding scheme, which generalizes transmit outage precoding (TOP) [4] in that multiple thresholds for the power normalization factor are used. We also describe how to choose the thresholds to optimize overall system performance. With multi-threshold TOP, the feedforward problem can be solved without noticeable performance degradation since there is only a finite number of power normalization factors (thresholds) and thus there is no receiver mismatch due to quantization errors.
- We show that multi-threshold TOP entails a very efficient implementation of the search for the perturbation vector that dominates the complexity at the base station. The receiver processing (including the decoding of the feedforward information) has extremely low complexity as it only involves a scaling, a modulo operation, and a slicing operation.
- We demonstrate analytically that multi-threshold TOP can achieve full diversity, even in the case of imperfect channel state information (CSI), whereas conventional precoding with finite-rate feedforward suffers from an error floor. This is corroborated by numerical simulations, which further reveal that the average transmit power of multi-threshold TOP is significantly smaller than that of conventional precoding.

The rest of the paper is organized as follows. In Section 2, we present the system model and the model for imperfect CSI. Section 3 discusses conventional VP precoding with finite-rate feedforward. Multi-threshold TOP is introduced and analyzed in Section 4. In Section 5 we present simulations results and Section 6 provides conclusions.

2. SYSTEM AND CSI MODEL

We consider a wireless multi-user downlink (see e.g. [1, 3]), in which a base station with M antennas transmits simultaneously to $K \leq M$ users, each equipped with a single receive antenna. In one time slot, user k receives $r_k = \mathbf{h}_k^{\mathrm{T}}\mathbf{x} + w_k$, where $\mathbf{h}_k$ denotes the MISO channel from the base station to user k, $\mathbf{x} = (x_1 \ldots x_M)^{\mathrm{T}}$ denotes the transmit vector, and w_k is additive circularly complex Gaussian noise. Collecting the receive values of all users in a receive vector $\mathbf{r} \triangleq (r_1 \ldots r_K)^{\mathrm{T}}$ yields the overall system model

$$\mathbf{r} = \mathbf{H}\mathbf{x} + \mathbf{w} \quad \text{with } \mathbf{H} = \big(\mathbf{h}_1 \ldots \mathbf{h}_K\big)^{\mathrm{T}} \qquad (1)$$

This work is supported by the STREP project MASCOT (IST-026905) within the Sixth Framework Programme of the European Commission.

and $\mathbf{w} \triangleq (w_1 \dots w_K)^{\mathrm{T}} \sim \mathcal{CN}(\mathbf{0}, \sigma^2\mathbf{I})$. The channel is modeled as block flat fading with i.i.d. $\mathcal{CN}(0,1)$ distribution for the elements of $\mathbf{H}$. We impose an *instantaneous* power constraint that requires

$$\|\mathbf{x}\|^2 \leq P\,,$$

which is well-suited for practical implementations.

2.1. Channel State Information

We assume that the base station has imperfect CSI corresponding to a noisy version of the channel matrix, i.e.,

$$\hat{\mathbf{H}} = \mathbf{H} + \mathbf{E}\,. \tag{2}$$

The CSI accuracy is characterized by the error matrix $\mathbf{E}$ which is assumed to be independent of $\mathbf{H}$. For simplicity, we model $\mathbf{E}$ as complex Gaussian with i.i.d. elements, i.e.,

$$\mathrm{vec}\{\mathbf{E}\} \sim \mathcal{CN}(\mathbf{0}, \eta\mathbf{I}) \quad \text{with} \quad \eta \triangleq \beta\rho^{-\alpha}. \tag{3}$$

Here, $\rho \triangleq P/\sigma^2$ denotes the nominal SNR and the parameters $\alpha \geq 0$ and $\beta > 0$ determine CSI accuracy. We note that the elements of the CSI matrix $\hat{\mathbf{H}}$ are hence i.i.d. $\mathcal{CN}(0, 1+\eta)$. The special case of perfect CSI at the base station corresponds to $\alpha \to \infty$. Two practically more relevant special cases are discussed in the following.

In *reciprocal systems*, the downlink and the uplink channel are equal. This allows the base station to estimate the channel matrix during uplink transmissions (e.g., via pilots sent by the users). In this case, $\mathbf{E}$ models channel estimation errors whose power depends inversely proportional on SNR. Such a scenario is captured by (3) with $\alpha = 1$.

In *non-reciprocal systems*, CSI feedback is required which entails two kinds of errors: (i) feedback delays can cause the CSI to be outdated (this depends on the channel's coherence time); (ii) finite-rate feedback requires CSI quantization and thus suffers from quantization noise. Both effects do not improve with increasing SNR, which amounts to (3) with $\alpha = 0$.

3. CONVENTIONAL VP PRECODING WITH FINITE-RATE FEEDFORWARD

3.1. Principle and Transmit-Side Processing

VP precoding [1–3] augments zero-forcing precoding with an additive perturbation of the data vector followed by appropriate power normalization, thereby enabling the users to perform data detection in a non-cooperative and low-complexity manner. Specifically, the transmit signal of conventional VP precoding [2] under imperfect CSI is given by

$$\mathbf{x} = \sqrt{\frac{P}{\Gamma(\hat{\mathbf{H}}, \mathbf{s})}}\, \hat{\mathbf{H}}^{\dagger}(\mathbf{s} + \tau\mathbf{z}^{\star})\,. \tag{4}$$

Here, $\hat{\mathbf{H}}^{\dagger} = \hat{\mathbf{H}}^{\mathrm{H}}(\hat{\mathbf{H}}\hat{\mathbf{H}}^{\mathrm{H}})^{-1}$ denotes the right pseudo inverse of $\hat{\mathbf{H}}$, $\mathbf{s} = (s_1 \dots s_k)^{\mathrm{T}} \in \mathcal{A}^K$ is the data vector with power-normalized elements ($\mathrm{E}\{|s_k|^2\} = 1$) from the symbol alphabet $\mathcal{A}$, and τ is a fixed real-valued parameter. The power normalization in (4) involves the *un-normalized* transmit power $\Gamma(\hat{\mathbf{H}}, \mathbf{s}) \triangleq \|\hat{\mathbf{H}}^{\dagger}(\mathbf{s} + \tau\mathbf{z}^{\star})\|^2$ and guarantees that the instantaneous power constraint is satisfied. The optimal perturbation vector that maximizes receive SNR equals

$$\mathbf{z}^{\star} = \arg\min_{\mathbf{z}\in\mathbb{G}^K} \left\|\hat{\mathbf{H}}^{\dagger}(\mathbf{s} + \tau\mathbf{z})\right\|^2. \tag{5}$$

Here, $\mathbb{G}^K$ is the set of Gaussian integer vectors.[1]

The power normalization factor $\Gamma(\hat{\mathbf{H}}, \mathbf{s})$ explicitly depends on the channel (estimate) and the data and needs to be known by all users in order to successfully recover their data symbols. A crucial aspect of VP precoding that has not been addressed up to now is the accurate feedforward of $\Gamma(\hat{\mathbf{H}}, \mathbf{s})$ to the individual users.

3.2. Finite-Rate Feedforward

Feedforward of the power normalization factor $\Gamma(\hat{\mathbf{H}}, \mathbf{s})$ for each time slot (i.e., for each data vector $\mathbf{s}$) is clearly undesirable. Hence, we consider a slight modification of VP precoding in which the same normalization factor $\tilde{\Gamma}(\hat{\mathbf{H}})$ is used for all data vectors within a block in order to reduce the feedforward overhead. To satisfy the instantaneous power constraint, $\tilde{\Gamma}(\hat{\mathbf{H}})$ has to be chosen as the maximum of all $\Gamma(\hat{\mathbf{H}}, \mathbf{s})$ within the block. The modified transmit signal then reads

$$\mathbf{x} = \sqrt{\frac{P}{\tilde{\Gamma}(\hat{\mathbf{H}})}}\, \hat{\mathbf{H}}^{\dagger}(\mathbf{s} + \tau\mathbf{z}^{\star})\,. \tag{6}$$

The power normalization factor $\tilde{\Gamma}(\hat{\mathbf{H}})$ is quantized with respect to a codebook $\mathcal{C} = \{\tilde{\gamma}_1, \dots, \tilde{\gamma}_L\}$ that is known by the receivers (we assume $0 < \tilde{\gamma}_1 < \tilde{\gamma}_2 < \cdots < \tilde{\gamma}_L$). This codebook can be designed e.g. using the Lloyd-Max [5] algorithm. The index l of the quantization level $\tilde{\gamma}_l = \mathcal{Q}_{\mathcal{C}}\{\tilde{\Gamma}(\hat{\mathbf{H}})\}$ is then transmitted to the individual users. Since VP precoding can *not* be used for that purpose, we propose to use TDMA and single-user beamforming with an m-ary symbol constellation, where the constellation size m is chosen depending on the SNR operating point. The users can detect the corresponding symbols within their dedicated time slots by simple quantization of the receive values. This feedforward scheme is very simple and effective, consumes $K\log_m(L)$ time-slots per block, and enables the receivers to recover $\tilde{\gamma}_l$ reliably.

3.3. Receiver Processing

With conventional VP, each user performs detection by appropriate scaling of the receive signal, $\tilde{r}_k \triangleq c\,r_k$, and applying a complex-valued modulo-τ operation (denoted $\mathcal{M}_\tau\{\cdot\}$) followed by quantization with respect to the symbol alphabet $\mathcal{A}$ (denoted $\mathcal{Q}_{\mathcal{A}}\{\cdot\}$) [1,2], i.e.,

$$\hat{s}_k = \mathcal{Q}_{\mathcal{A}}\left\{\mathcal{M}_\tau\{\tilde{r}_k\}\right\}\,. \tag{7}$$

[1] The set $\mathbb{G}$ of Gaussian integers comprises all complex numbers with integer real and imaginary parts.

While in an idealized scenario $c = \sqrt{\tilde{\Gamma}(\hat{\mathbf{H}})/P}$, with finite-rate feedforward (assumed perfect) the scaling factor will be $c = \sqrt{\tilde{\gamma}_l/P}$ such that the receivers cannot fully compensate for $\tilde{\Gamma}(\hat{\mathbf{H}})$. Inserting (6) into (1) then leads to

$$\tilde{r}_k = \sqrt{\frac{\tilde{\gamma}_l}{P}}\, r_k = \sqrt{\frac{\tilde{\gamma}_l}{\tilde{\Gamma}(\hat{\mathbf{H}})}}\,(s_k + \tau z_k^\star) + \sqrt{\frac{\tilde{\gamma}_l}{P}}\, w_k. \qquad (8)$$

The mismatch

$$\frac{\tilde{\gamma}_l}{\tilde{\Gamma}(\hat{\mathbf{H}})} \neq 1$$

will result in additional errors. Specifically, $\frac{\tilde{\gamma}_l}{\tilde{\Gamma}(\hat{\mathbf{H}})}$ can become arbitrarily small (for $\tilde{\Gamma}(\hat{\mathbf{H}}) > \tilde{\gamma}_L$) and arbitrarily large (for $\tilde{\Gamma}(\hat{\mathbf{H}}) < \tilde{\gamma}_1$) since $\tilde{\Gamma}(\hat{\mathbf{H}})$ is a continuous random variable on $\mathbb{R}^+$ and the quantization codebook $\mathcal{C}$ has finite size. These events happen with non-zero probability independent of the SNR, thus causing errors even if there is no noise. It follows that conventional VP precoding with finite-rate feedforward features an error floor that is determined by the codebook size.

4. MULTI-THRESHOLD TOP

4.1. Basic Principle

In order to circumvent the error floor of conventional VP precoding with finite-rate feedforward, we propose a new precoding scheme that extends *transmit outage precoding (TOP)* from [4] by using multiple thresholds (power normalization factors). Multi-threshold TOP does not feature a mismatch between the power normalization factor at the base station and the re-scaling at the receivers. Furthermore, it avoids transmissions at all when the available power does not suffice to perform channel pre-equalization.

Consider a set of L normalization factors/thresholds $\mathcal{G} \triangleq \{\gamma_1, \dots, \gamma_L\}$ sorted according to $0 < \gamma_1 < \gamma_2 < \cdots < \gamma_L$ and known to the users (the scheme in [4] is re-obtained with $L = 1$). For simplicity of presentation, we define $\gamma_0 = 0$. With multi-threshold TOP, the transmit signal is given by

$$\mathbf{x} = \begin{cases} \sqrt{\frac{P}{\gamma_l}}\, \hat{\mathbf{H}}^\dagger(\mathbf{s} + \tau\mathbf{z}^\star) & \text{for } \gamma_{l-1} < \tilde{\Gamma}(\hat{\mathbf{H}}) \leq \gamma_l \\ \mathbf{0} & \text{for } \tilde{\Gamma}(\hat{\mathbf{H}}) > \gamma_L\,, \end{cases} \qquad (9)$$

Note that we abstain from transmitting whenever the channel quality is very poor in the sense that $\tilde{\Gamma}(\hat{\mathbf{H}}) > \gamma_L$. This event, denoted $\mathcal{O}$, will be termed a "transmit outage." The rationale is that in case of such an event no transmit power is wasted since reliable reception is highly unlikely anyway. Even in the case of transmission ($\tilde{\Gamma}(\hat{\mathbf{H}}) \leq \gamma_L$), the transmit signal in (9) allows for significant power savings since $\|\mathbf{x}\|^2 \leq \frac{P}{\gamma_l}\tilde{\Gamma}(\hat{\mathbf{H}}) \leq P$ (see also Section 5).

The index l of the power normalization factor γ_l can be directly fed forward to the receivers. To this end, we use TDMA-based single-user beamforming with an m-ary constellation like with conventional VP. In the case of an outage, the feedforward of the index l is not necessary since reliable data reception is impossible anyway.

The receiver processing for multi-threshold TOP is the same as with conventional precoding. However, assuming perfect reception of γ_l and perfect CSI, in this case the users indeed observe noisy versions of their data symbol, i.e., in the no-outage case there is

$$\tilde{r}_k = \sqrt{\frac{\gamma_l}{P}}\, r_k = s_k + z_k^\star + \sqrt{\frac{\gamma_l}{P}}\, w_k \qquad (10)$$

A decision is then obtained by modulo and slicing operations according to (7). Clearly, in the absence of noise, the data symbols can be perfectly recovered from (10) and hence there is no error floor (the probability or an outage can be made to go to zero with increasing SNR, see below).

4.2. Performance Analysis

We next optimize the error probability with respect to $\mathcal{G}^\star$ and present results on the diversity order of multi-threshold TOP.

Optimal threshold set. The optimal threshold set is given by

$$\mathcal{G}^\star \triangleq \{\gamma_1^\star, \dots, \gamma_L^\star\} = \arg\min_{\mathcal{G} \subset \mathbb{R}_+^L} \Pr\{\mathcal{E}_s; \mathcal{G}\}\,, \qquad (11)$$

where $\mathcal{E}_s$ denotes the event for a symbol error whose probability equals

$$\Pr\{\mathcal{E}_s; \mathcal{G}\} = \tfrac{1}{2}\Pr\{\mathcal{O}\} + \sum_{l=1}^{L} \Pr\{\mathcal{E}_s | \mathcal{P}_l\} \Pr\{\mathcal{P}_l\} \qquad (12)$$

with $\mathcal{P}_l \triangleq \{\gamma_{l-1} < \tilde{\Gamma}(\hat{\mathbf{H}}) \leq \gamma_l\}$. The probabilities $\Pr\{\mathcal{O}\}$, $\Pr\{\mathcal{E}_s|\mathcal{P}_l\}$, and $\Pr\{\mathcal{P}_l\}$ can be computed by means of Monte-Carlo simulations and the optimal threshold set can be obtained by mean of a numerical optimization. We emphasize that $\mathcal{G}^\star$ will depend on the SNR ρ.

Diversity. We next discuss the diversity order of multi-threshold TOP, defined as

$$d \triangleq -\lim_{\rho\to\infty} \frac{\log \Pr\{\mathcal{E}_s; \mathcal{G}^\star\}}{\log \rho}. \qquad (13)$$

Since the derivation of d is largely parallel to [6], we provide only as much information as required to adapt the proof from [6] to the present setup. Lets consider a specific threshold set where $\gamma_L = c\rho^\kappa$ with $c > 0$ and $\kappa > 0$. We have

$$\begin{aligned} \Pr\{\mathcal{E}_s; \mathcal{G}^\star\} &\leq \Pr\{\mathcal{E}_s; \mathcal{G}\} \\ &\leq \Pr\{\tilde{\Gamma}(\hat{\mathbf{H}}) > \gamma_L\} + L \Pr\{\mathcal{E}_s | \tilde{\Gamma}(\hat{\mathbf{H}}) \leq \gamma_L\} \end{aligned}$$

where the first inequality holds due to the optimality of $\mathcal{G}^\star$ and the second follows from (12). It can then be shown that $\Pr\{\mathcal{E}_s|\tilde{\Gamma}(\hat{\mathbf{H}}) \leq \gamma_L\}$ decays exponentially fast for $\kappa <$

$\min(\alpha,1)$ whereas it is strictly bounded away from zero for $\kappa \geq \min(\alpha,1)$. Using the bounds for $\Gamma(\hat{\mathbf{H}},\mathbf{s})$ from [6], which are independent of $\mathbf{s}$ and hence also apply to $\tilde{\Gamma}(\hat{\mathbf{H}})$, the outage probability can be shown to scale according to $\Pr\{\tilde{\Gamma}(\hat{\mathbf{H}}) > \gamma_L\} \doteq \rho^{-\kappa M}$. In view of the restriction regarding κ, the resulting upper bound implies that the diversity order of multi-threshold top is lower bounded by $M\min(\alpha,1)$. The lower bound is however identical to the diversity order of conventional VP precoding under a short-term or instantaneous power constraint [6]. It can also be shown that multi-threshold TOP cannot outperform conventional VP precoding where the power normalization factor is perfectly known to the receivers. We conclude that the diversity order (13) of multi-threshold TOP equals

$$d = M\min(\alpha,1)\,.$$

In particular, while the diversity order depends on the CSI accuracy parameter α, we have $d > 0$ and hence no error floor unless $\alpha = 0$, reflecting the fact that the finite-rate feedforward is unproblematic with multi-threshold TOP.

4.3. Low-Complexity Variant

One of the advantages of VP precoding is that most of the computational complexity is shifted to the base station, whereas the receiver complexity is extremely low. The base station complexity in turn is dominated by the search for the optimal perturbation vector (cf. (5)) that minimizes the unnormalized transmit power $\|\hat{\mathbf{H}}^\dagger(\mathbf{s}+\tau\mathbf{z})\|^2$. This minimization problem is an integer least-squares problem whose complexity in general is exponential in the number of users K. A promising algorithm to solve (5) is the sphere decoding algorithm [2, 7] (in this context also referred to as *sphere encoding* [2]), which, however, is still exponentially complex [8] (in the worst case and on average). Using the QR-decomposition $-\tau\hat{\mathbf{H}}^\dagger = \mathbf{QR}$ with the $M\times K$ matrix $\mathbf{Q}$ satisfying $\mathbf{Q}^H\mathbf{Q} = \mathbf{I}$ and the $K\times K$ upper triangular matrix $\mathbf{R}$, we can write

$$\|\hat{\mathbf{H}}^\dagger(\mathbf{s}+\tau\mathbf{z})\|^2 = \|\mathbf{Q}\mathbf{Q}^H\hat{\mathbf{H}}^\dagger\mathbf{s} - \mathbf{QRz})\|^2 = \|\mathbf{a}-\mathbf{Rz}\|^2,$$

where $\mathbf{a} = \mathbf{Q}^H\hat{\mathbf{H}}^\dagger\mathbf{s}$. The upper triangular matrix $\mathbf{R}$ induces a tree, which is traversed by the sphere encoder in a branch-and-bound manner to find the optimal $\mathbf{z}$. In the tree traversal, only nodes corresponding to solutions that lie within a hypersphere of radius R about the center point $\mathbf{a}$ are visited. We use the Schnorr-Euchner strategy [7, 9] which does not require an initial radius to be set. However, a given initial R has a crucial impact on the complexity, measured in terms of the number of nodes visited by the sphere encoder.

We propose a sphere encoder variant which is suited for multi-threshold TOP and uses an early termination idea resulting in significant complexity savings with moderate performance loss. Rather than performing the costly search for the optimal perturbation vector, the main idea is to terminate the search as soon as perturbation vectors $\bar{\mathbf{z}} \in \mathbb{G}^K$ for all $\mathbf{s}$ within the block are found such that $\|\hat{\mathbf{H}}^\dagger(\mathbf{s}+\tau\bar{\mathbf{z}})\|^2 \leq \gamma_L$ and thus transmission is possible (i.e., a transmit outage is avoided). The normalization factor $\tilde{\Gamma}(\hat{\mathbf{H}})$ in the multi-threshold TOP scheme is then replaced with the maximum of $\|\hat{\mathbf{H}}^\dagger(\mathbf{s}+\tau\bar{\mathbf{z}})\|^2$ within the block, denoted $\bar{\Gamma}(\hat{\mathbf{H}})$. This approach dramatically reduces the sphere encoder complexity (measured in terms of the number of nodes in the tree that are visited). On the other hand there is $\bar{\Gamma}(\hat{\mathbf{H}}) \geq \tilde{\Gamma}(\hat{\mathbf{H}})$, which entails a certain performance loss (see Section 5).

The search for $\bar{\mathbf{z}}$ is most easily accomplished by choosing the initial radius for sphere encoding as $\sqrt{\gamma_L}$ (cf. (9)) and terminating as soon as the first leaf node is reached. If the sphere with radius $\sqrt{\gamma_L}$ does not contain any perturbation vector, there is a transmit outage which is implicitly recognized by the sphere precoder.

We note that the threshold optimization diversity analysis of multi-threshold TOP can be straightforwardly extended to the above low-complexity variant.

5. SIMULATION RESULTS

We present simulation results for $K = 6$ users and a base station with $M = 6$ antennas using a 4-QAM symbol alphabet. For feedforward transmission we used BPSK, which consumes $6B$ time slots ($B = \log_2(L)$ is the number of feedforward bits), whereas 90 data symbols were transmitted within each block. The channel was i.i.d. Rayleigh fading.

Fig. 1(a) shows the bit error rate (BER) versus nominal SNR $\rho = P/\sigma^2$ for conventional VP precoding, multi-threshold TOP (labeled 'MTOP'), and the low-complexity variant of multi-threshold TOP ('MTOP–LC'), all with $B = 2$ bits feedforward and perfect CSI. MTOP and MTOP-LC use thresholds optimized according to (11). The BER of "genie" scheme using conventional precoding and perfect knowledge of $\tilde{\Gamma}(\hat{\mathbf{H}})$ at the receivers is plotted as ultimate benchmark. Conventional precoding is seen to suffer indeed from an error floor. In contrast, multi-threshold TOP and its low-complexity variant achieve full diversity ($d = M = 6$), with an SNR gap of about 2.5 dB between the two.

Fig. 1(b) depicts similar results for the case of imperfect CSI ($\alpha = \beta = 1$) and $B = 1$ bit feedforward. Here, the error floor of conventional precoding is noticeable larger and the SNR gap between multi-threshold TOP and its low-complexity variant is only about 1.7 dB.

Fig. 1 does not account for the power savings of MTOP(-LC). The latter are illustrated in Fig. 2, which depicts the average transmit power (normalized by P) versus SNR for conventional precoding and the low-complexity variant of multi-threshold TOP, again assuming perfect CSI. MTOP and MTOP-LC are seen to spend much less transmit power than conventional precoding, particularly at high SNR. Furthermore, the power savings decrease with increasing number of thresholds. With $B = 1$ ($L = 2$), MTOP-LC uses still

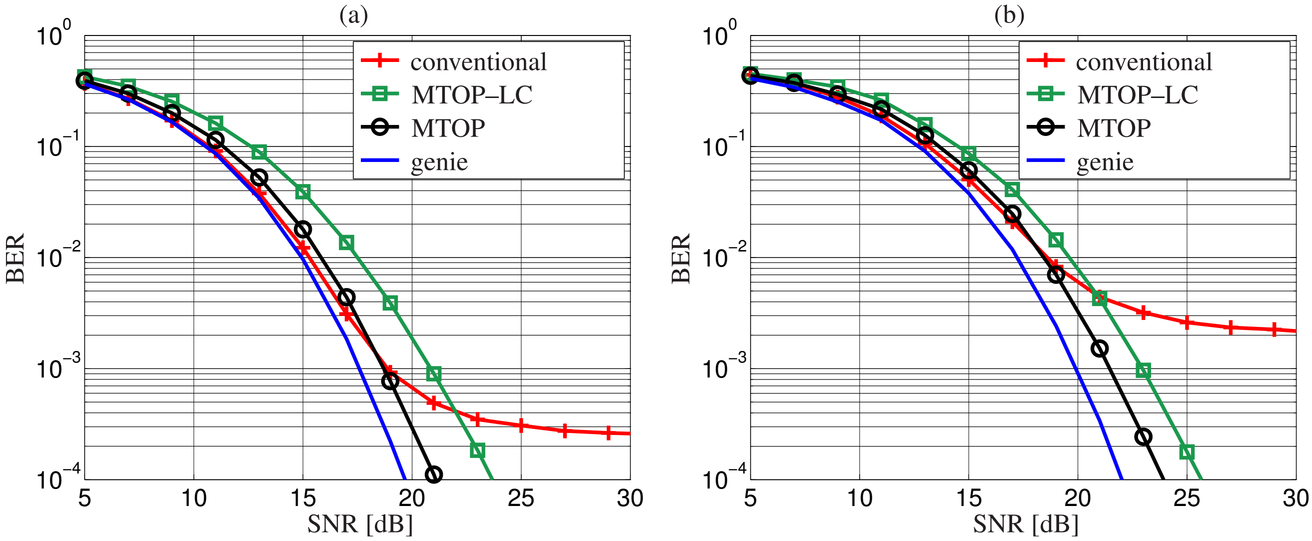

Fig. 1. *BER vs. SNR for conventional precoding, multi-threshold TOP ('MTOP') and its low-complexity variant ('MTOP–LC.') for (a) perfect CSI and 2 bit feedforward and (b) imperfect CSI ($\beta = \alpha = 1$) and 1 bit feedforward.*

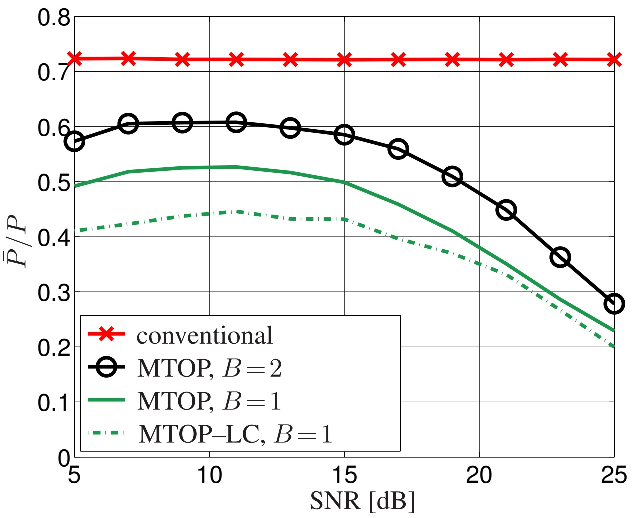

Fig. 2. *Normalized average transmit power vs. SNR for conventional precoding, MTOP, and MTOP-LC with 1 bit and 2 bit feedforward.*

less average power than MTOP. This can be explained by the fact that MTOP-LC results in additional symbol errors due to increased noise enhancement, which in turn results in smaller optimal thresholds $\gamma_l^\star$. Smaller $\gamma_L^\star$ results in more transmit outages and hence in smaller average transmit power.

6. CONCLUSIONS

In this paper, we considered a realistic variant of vector perturbation precoding, which is augmented by finite-rate feedforward of the quantized power normalization factor. Since this scheme was seen to feature an error floor, we proposed multi-threshold transmit outage precoding, which uses identical discrete power normalization factors at the base station and at the receivers. In addition, it avoids transmitting when the available power is not sufficient to perform channel equalization at the transmit side. We further provided a low-complexity variant of multi-threshold transmit outage precoding that uses a simplified sphere encoding strategy. It was observed that the proposed precoding scheme requires significantly smaller average transmit power and exploits all the available diversity (i.e., no error floor).

REFERENCES

[1] C. B. Peel, B. M. Hochwald, and A. L. Swindlehurst, "A vector-perturbation technique for near-capacity multiantenna multiuser communication - Part I: Channel inversion and regularization," *IEEE Trans. Comm.*, vol. 53, pp. 195–202, Jan. 2005.

[2] B. M. Hochwald, C. B. Peel, and A. L. Swindlehurst, "A vector-perturbation technique for near-capacity multiantenna multiuser communication - Part II: Perturbation," *IEEE Trans. Comm.*, vol. 53, pp. 537–544, March 2005.

[3] C. Windpassinger, R. F. H. Fischer, T. Vencel, and J. B. Huber, "Precoding in multiantenna and multiuser communications," *IEEE Trans. Wireless Comm.*, vol. 3, pp. 1305–1316, July 2004.

[4] J. Maurer, J. Jaldén, and G. Matz, "Transmit outage precoding with imperfect channel state information under an instantaneous power constraint," in *Proc. IEEE SPAWC'08*, (Recife, Brasil), pp. 66–70, July 2008.

[5] A. Gersho and R. M. Gray, *Vector Quantization and Signal Compression*. Boston: Kluwer, 1992.

[6] J. Jaldén, J. Maurer, and G. Matz, "On the diversity order of vector perturbation precoding with imperfect channel state information," in *Proc. IEEE SPAWC'08*, (Recife, Brasil), pp. 211–215, July 2008.

[7] E. Agrell, T. Eriksson, A. Vardy, and K. Zeger, "Closest point search in lattices," *IEEE Trans. Inf. Theory*, vol. 48, pp. 2201–2214, Aug. 2002.

[8] J. Jaldén and B. Ottersten, "On the complexity of sphere decoding in digital communications," *IEEE Trans. Signal Processing*, vol. 53, pp. 1474–1484, Apr. 2005.

[9] C. P. Schnorr and M. Euchner, "Lattice basis reduction: Improved practical algorithms and solving subset sum problems," *Mathematical Programming*, vol. 66, pp. 181–199, Aug. 1994.